111. Estimation of grassland structure as a proxy for biomass under free-field photovoltaic systems using handheld SLAM LiDAR

C. Hütt^{1,*}, J. Isselstein^{2,3}, A. Jenal⁴, F. Kunz², L. Vehlken¹, J. Wolf¹, L. Zinken², and D. Hamidi²

¹GIS & RS Group, Institute of Geography, University of Cologne, Cologne, Germany; * christoph. huett@uni-koeln.de

Abstract

In free-field photovoltaic (FFPV) systems, grassland integration offers dual land use, but measuring vegetation beneath photovoltaic (PV) modules is challenging. Traditional methods like the rising plate meter (RPM) lack spatial continuity, and remote sensing often struggles to capture the area below the modules. Here, a handheld simultaneous localization and mapping (SLAM) light detection and ranging (LiDAR) system captured high-resolution 3D data of grass swards in an FFPV site. LiDAR-derived canopy height metrics correlated strongly with RPM measurements (R^2 up to 0.88 in open areas, 0.75 under PV modules). Handheld SLAM LiDAR thus provides an efficient means to assess grass structure in complex environments, supporting precision pasture management and environmental monitoring.

Keywords: free-field photovoltaic, grassland biomass estimation, LiDAR, solar park monitoring, vegetation structure

Introduction

The expansion of free-field photovoltaic (FFPV) systems over grasslands has created novel opportunities for dual land use, combining renewable energy generation with sustainable agricultural practices such as livestock grazing (Hamidi *et al.*, 2024; Zahrawi and Aly, 2024). This co-use of land for energy and pasture management is promising for regions aiming to balance environmental and agricultural goals (Hamidi *et al.*, 2024), but it also introduces unique challenges in assessing vegetation growth beneath photovoltaic modules (Soto-Gómez, 2024). Accurately quantifying biomass in these partially shaded areas is essential for evaluating how PV panels influence both the agronomic value of the pasture and its ecological conditions.

Traditional ground-based techniques for measuring biomass, such as the rising plate meter (RPM) and sward stick, offer only localized measurements that fail to capture the spatially continuous data (Bareth and Schelberg, 2018). Similarly, remote sensing methods commonly used in agricultural biomass estimation, such as satellite and aerial imaging, are limited under PV modules because of shading effects that reduce visibility and accuracy in obstructed areas (Lu, 2006).

Light detection and ranging (LiDAR) scanning, particularly when mounted on uncrewed aerial vehicles (UAVs), has recently emerged as a spatially consistent and efficient tool for estimating grassland biomass (Wang *et al.*, 2017). The LiDAR scanners generate three-dimensional point clouds by emitting laser beams and measuring their return time. By capturing the canopy's three-dimensional structure, these point clouds facilitate the estimation of vertically dependent grassland traits, including biomass.

Handheld LiDAR systems, unlike UAV-mounted LiDAR, enable direct data collection beneath PV modules, avoiding issues such as obstructions and flight clearance requirements. Additionally,

 ² Department of Crop Sciences, Grassland Science, University of Göttingen, Göttingen, Germany
 ³Centre for Biodiversity and Sustainable Land Use, University of Göttingen, Göttingen, Germany
 ⁴AMLS – Application Center for Machine Learning and Sensor Technologies, University of Applied Sciences Koblenz, Koblenz, Germany

simultaneous localization and mapping (SLAM) technology ensures precise mapping without reliance on GNSS, making it effective in areas with poor signal reception (Wei *et al.*, 2024). De Nobel *et al.* (2023) have already demonstrated the potential of using handheld SLAM LiDAR scanners to estimate grassland biomass. Handheld SLAM LiDAR systems seem particularly suited for environments with limited accessibility, such as shaded areas beneath photovoltaic (PV) modules. This study presents a case where a handheld SLAM LiDAR system was used to analyse grass sward structure as a proxy for biomass under PV modules, enabling continuous, high-resolution data collection of vertical vegetation structures.

Study area and methods

Study area

The study area was in an FFPV in Lottorf, in Northern Germany (54°26′37″N, 9°34′08″E), built on a peat grassland. This park features single-axis sun-tracking modules, posing unique scanning challenges due to their dynamic positioning (Figure 1).

Data acquisition

On 27 May 27 a Hovermap (Hovermap ST, Emesent, Brisbane, QLD, Australia) SLAM LiDAR scanner in a handheld configuration was used to scan an area of approximately 0.3 ha. During the 953 s scanning period, 78 million points were recorded (Figure 2). Six round plate targets, each 0.5 m in diameter, and made of red and white reflective foil, were laid out as ground control points (GCP), as shown in Figure 1. Their positions were measured using a real-time kinematic differential GPS (GR-5, Topcon, Tokyo, Japan) for accurate spatial referencing.

On the following day (28 May 2024), ground-based measurements were collected to serve as reference data. These included rising plate meter (RPM) measurements at various positions under and around the modules (n=20), as well as in the open area adjacent to the modules (n=34). The RPM is a device with a 15 cm radius plate that compresses the grass canopy, providing a measurement that reflects compressed sward height. Along two 10 m transects, sward stick measurements were conducted at 0.2 m intervals and RPM measurements at 0.3 m intervals. In contrast to the RPM, the Sward Stick measures the maximum plant height at a specific point using a sliding viewfinder that is lowered until it makes contact with the first plant part. The RPM measurements at various positions and the start and end points of the transects were also measured using the same differential GPS as above. However, directly under the modules, GNSS measurements were not possible. To estimate these positions, straight lines and distances from measurable points were determined using a ruler. This method approximated the positions beneath the panels, compensating for GNSS limitations.

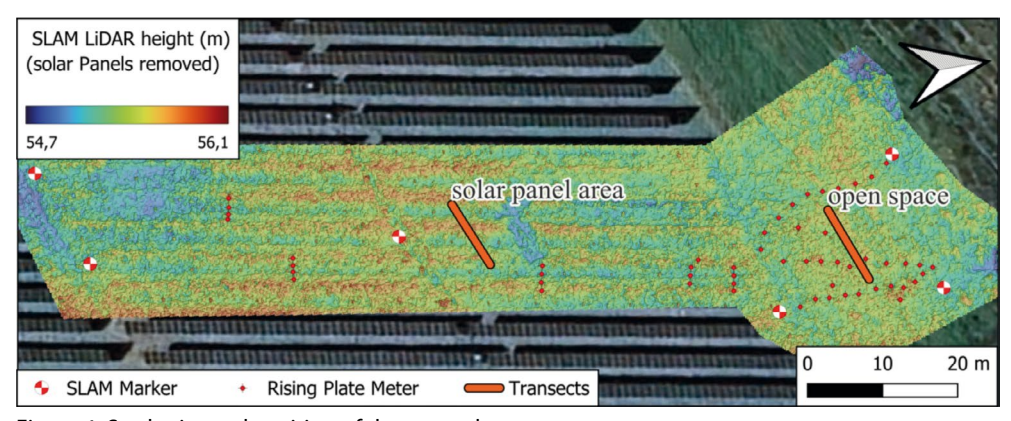


Figure 1. Study site and position of the ground measurements.

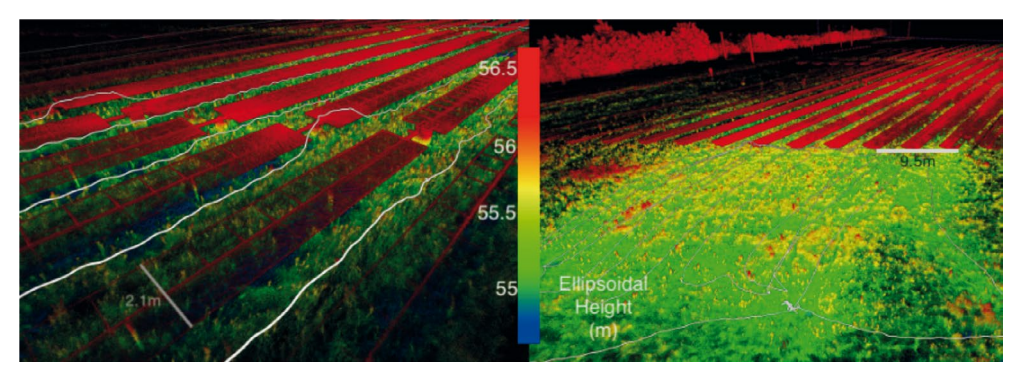


Figure 2. Visualization of the point cloud (coloured by height) acquired with the Hovermap ST and the trajectory (white) representing the path walked while carrying the device. The left side shows the area under the panels, while the right side depicts the open space area.

Processing of the SLAM LIDAR point cloud

The derived point cloud was processed in Aura (Version 1.8) using the measured positions of the GCPs for georeferencing. The forest preset processing option was selected, as it proved most effective for generating a consistent point cloud in this environment. Subsequent steps were carried out in R (4.3.2) using the lidR package (4.1.1) and included noise filtering, classification of ground points, and normalization. During normalization, all points were adjusted to have elevations relative to the ground surface, effectively setting the ground level to zero. This allows for accurate analysis of the canopy's vertical structure. Furthermore, the point cloud was manually segmented to identify and exclude all points corresponding to the PV modules, ensuring they were not included in subsequent analyses (Figure 3).

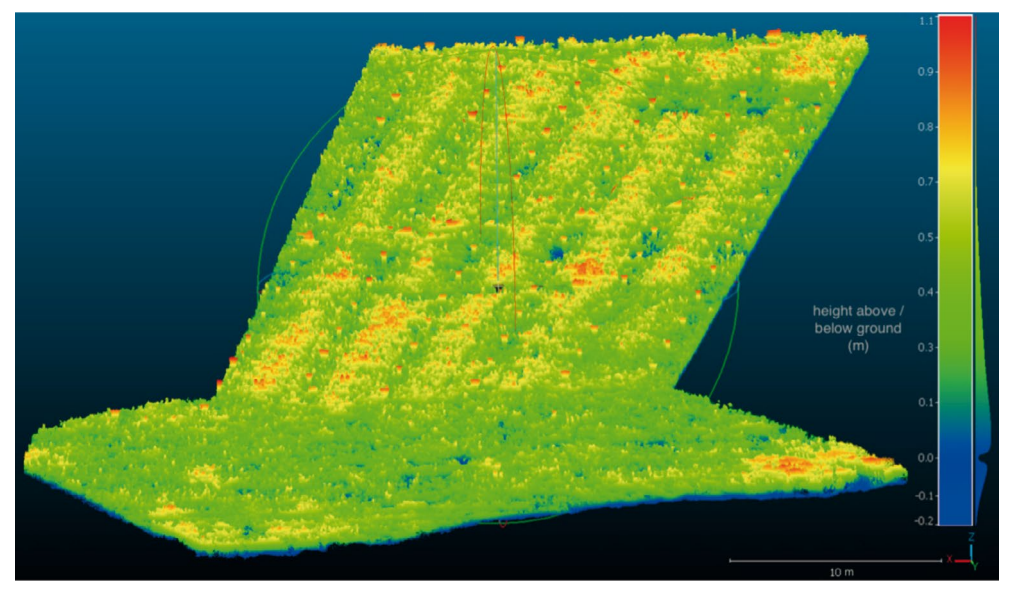


Figure 3. Visualization of the normalized point cloud with the points representing the PV modules removed.

To extract LiDAR metrics corresponding to the RPM measurements distributed across the study area, circular buffer zones were created with a radius of 0.3 m around each measurement point. Along the transects, buffers of 0.05 m were created at every 0.1-m interval. In this study, the following LiDAR metrics (Hütt *et al.*, 2023) were calculated for each observation area: the minimum, maximum, mean, and the 25th, 50th, 75th, 90th, and 99th percentiles of the LiDAR-derived canopy heights.

Results

As illustrated in Figure 4, the transect profiles reveal correspondences among the measurements obtained from the RPM, sward stick, and the SLAM LiDAR. For example, a notable peak is observed at approximately 8 m along the transect in the area beneath the solar panels. The sward stick profiles often display patterns that closely resemble the 95th percentile of the LiDAR-derived canopy heights. In contrast, the RPM measurements align more closely with the lower percentiles of the LiDAR data. However, in many cases, peaks observed in the Sward Stick measurements are not fully captured by the LiDAR data, and the characteristic peak at around 6 m appears to be shifted by a few centimetres. Furthermore, it becomes apparent that the sward exhibits high spatial variability, which seems to be more pronounced in the areas beneath the PV modules.

Figure 5 illustrates the relationship between compressed sward height, measured with the RPM, and LiDAR-derived metrics at the 25th, 50th, and 90th quantiles for open spaces (blue) and PV module areas (orange). The regression lines and R^2 values reveal stronger correlations in open spaces compared to PV module areas, particularly for the 25th and 50th quantiles. Interestingly, R^2 values improve when the data from open spaces and PV module areas are analysed separately, emphasizing distinct relationships in these environments. The regression lines for PV module areas are consistently shifted upward, indicating that LiDAR-derived canopy heights are higher for the same RPM values under PV modules. In contrast, the 90th quantile shows weaker overall correlations, reflecting greater variability in this metric.

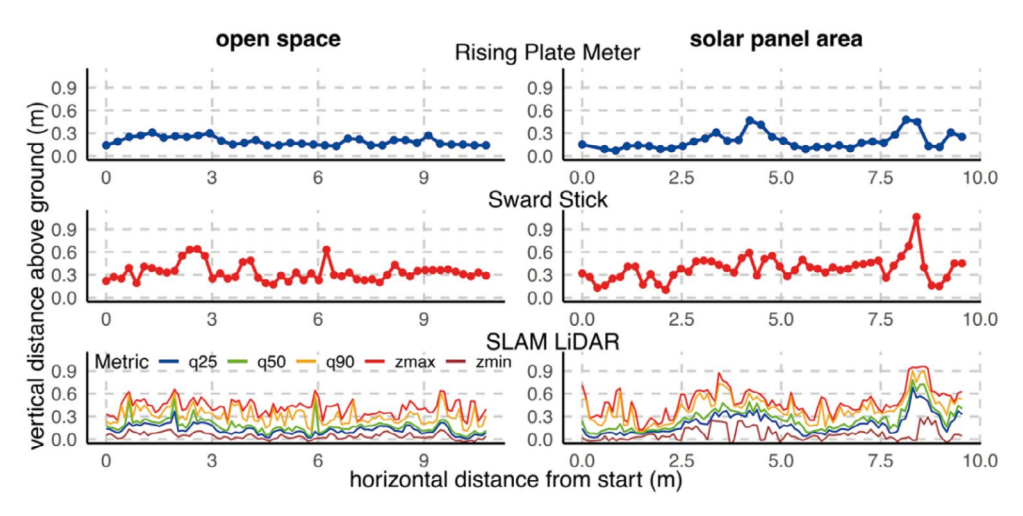


Figure 4. RPM, sward stick, and SLAM LIDAR measurements along two transects: one beneath the photovoltaic (PV) modules ("solar panel area", right) and one in open space unaffected by the PV modules (left).

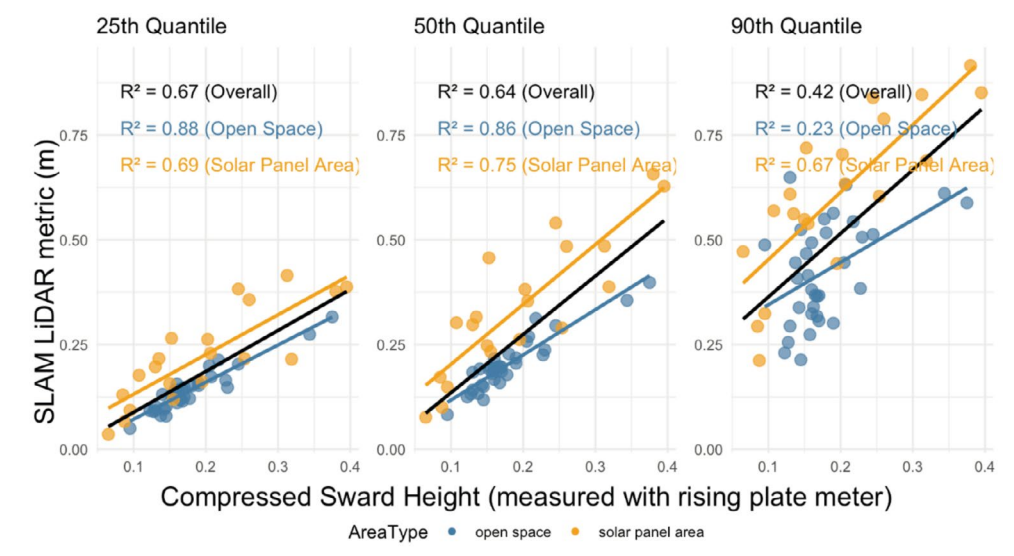


Figure 5. Relationship between compressed sward height (measured with a rising plate meter) and SLAM LiDAR metrics at the 25th, 50th, and 90th quantiles. Regression lines and R^2 values are shown for overall data (black), open space (blue), and solar panel areas (orange).

Discussion

This study highlights the utility of handheld SLAM LiDAR for capturing the 3D structure of grass swards, offering insights into vegetation height distribution in both open spaces and areas beneath PV modules. In open space areas, the 25th quantile of LiDAR-derived canopy height showed a strong correlation with RPM measurements (R^2 =0.88). While the agreement decreased under the PV modules, the 50th quantile still demonstrated a respectable R^2 of 0.75. These results align with those of de Nobel *et al.* (2023), who observed similar correlations between LiDAR metrics and RPM measurements, which are widely known as proxies for biomass.

The observed increase in R^2 values when differentiating between open spaces and areas beneath PV modules suggests that shading from the panels significantly impacts grass morphology and structural characteristics. This effect parallels patterns reported in silvopastoral systems, where tree canopies create sunlight deficiencies similar to those caused by the PV modules in the present study. Shading from PV modules may induce grass adaptations such as leaf elongation and increased specific leaf area, while reducing tiller production and altering biomass allocation patterns (Pontes $et\ al.$, 2017). These structural changes likely influence the relationship between RPM measurements, as proxies for biomass, and LiDAR-derived canopy height metrics, underscoring the necessity to account for shading effects introduced by the PV modules.

In the context of FFPV, particularly beneath the PV modules, where other surveying methods such as multispectral imaging (e.g., Lussem *et al.*, 2022) are ineffective due to obstructions, handheld SLAM LiDAR presents notable advantages. By capturing fine-scale variation in shaded or obstructed zones, it enables a more precise evaluation of how localized shading influences pasture growth. In this way, SLAM LiDAR provides a promising tool to assess the implications of solar panels on grass swards, potentially enhancing both understanding and management of environmental impacts. Although the results are preliminary and require further validation, the efficiency of SLAM LiDAR in capturing detailed spatial information underscores its potential utility in such complex environments.

However, the transect measurements revealed that the heterogeneity of the study area occurs on very small spatial scales, often within decimetres. This emphasizes the necessity for extremely precise localization of measurement points to ensure direct comparability between different methods. Achieving the required positional accuracy is significantly impeded by poor GNSS reception, especially beneath the PV modules. Additionally, the high costs associated with advanced equipment necessary for precise positioning and data collection present substantial limitations. These factors represent potential sources of error and should be considered when interpreting the results. To enhance spatial accuracy, alternative positioning solutions or the use of UAV-based remote sensing methods like UAV-based LiDAR or very oblique imaging could be explored to capture data under the PV modules.

Conclusions

In summary, the study demonstrated the potential of handheld SLAM LiDAR as an effective tool for assessing grass canopy structures in FFPV systems, particularly in shaded areas where traditional methods are limited. The significant differences in R^2 values between open and shaded areas highlighted the impact of PV modules -induced shading on grass morphology, necessitating adjustments in measurement approaches. Future research should focus on improving positional accuracy in challenging environments and validating SLAM LiDAR methodologies through destructive biomass sampling to strengthen the correlation between LiDAR metrics and actual biomass. Additionally, exploring UAV-based LiDAR systems could provide an effective means of capturing high-resolution spatial data, including areas beneath PV modules.

Acknowledgements

We thank the Bundesverband Neue Energiewirtschaft e.V. (BNE) for their support and Dag Frerichs and Holger Reimer for their assistance during the fieldwork.

References

- Bareth, G., & Schellberg, J. (2018). Replacing manual rising plate meter measurements with low-cost UAV-derived sward height data in grasslands for spatial monitoring. PFG–Journal of Photogrammetry, Remote Sensing and Geoinformation Science, 86, 157–168.
- de Nobel, J.S., Rijsdijk, K.F., Cornelissen, P., & Seijmonsbergen, A.C. (2023). Towards prediction and mapping of grassland aboveground biomass using handheld LiDAR. Remote Sensing, 15(7), 1754.
- Hamidi, D., Sieve, F., Siede, C., Wilms, L., Zinken, L., Kunz, F., ..., & Isselstein, J. (2024). Solargrazing spatial distribution of sheep in free-field-photovoltaic systems on grassland. Grassland Science in Europe, 29, 452–454.
- Hütt, C., Bolten, A., Hüging, H., & Bareth, G. (2023). UAV LiDAR metrics for monitoring crop height, biomass and nitrogen uptake: a case study on a winter wheat field trial. PFG–Journal of Photogrammetry, Remote Sensing and Geoinformation Science, 91(2), 65–76.
- Lu, D. (2006). The potential and challenge of remote sensing-based biomass estimation. International Journal of Remote Sensing, 27(7), 1297–1328.
- Lussem, U., Bolten, A., Kleppert, I., Jasper, J., Gnyp, M. L., Schellberg, J., & Bareth, G. 2022. Herbage mass, N concentration, and N uptake of temperate grasslands can adequately be estimated from UAV-based image data using machine learning. Remote Sensing, 14(13), 3066.
- Pontes, L.S., Carpinelli, S., Stafin, G., Porfirio-da-Silva, V., and Santos, B.R.C. (2016). Relationship between sward height and pasture biomass for integrated crop-livestock systems with trees. Japanese Society of Grassland Science, 63, 29-35.

- Soto-Gómez, D. (2024). Integration of crops, livestock, and solar panels: A review of agrivoltaic systems. Agronomy 14(8), 1824.
- Wang, D., Xin, X., Shao, Q., Brolly, M., Zhu, Z., & Chen, J. (2017). Modeling aboveground biomass in Hulunber grassland ecosystem by using unmanned aerial vehicle discrete lidar. Sensors, 17(1), 180.
- Wei, P., Fu, K., Villacres, J., Ke, T., Krachenfels, K., Stofer, C.R., ..., & Kong, Z. (2024). A compact handheld sensor package with sensor fusion for comprehensive and robust 3D mapping. Sensors, 24(8), 2494.
- Zahrawi, A.A., & Aly, M.A. (2024). A review of agrivoltaic systems: Addressing challenges and enhancing sustainability. Sustainability, 16(18), 8271.